

## Supporting Information

### **Superhydrophobic coating with micro- and nano-sized MnO<sub>2</sub>/PDMS composite structure for passive anti-icing/active de- icing and photothermal applications**

Jialun Li<sup>1</sup>, Fei Yu<sup>1</sup>, Yi Jiang<sup>2</sup>, Liying Wang<sup>1</sup>, Yaodong Liu<sup>1</sup>, Xijia Yang<sup>1</sup>, Xuesong Li<sup>1\*</sup>, Wei  
Lü<sup>1,3\*</sup>

<sup>1</sup>Key Laboratory of Advanced Structural Materials, Ministry of Education & Advanced Institute of Materials Science, Changchun University of Technology, Changchun 130012, People's Republic of China

<sup>2</sup>School of Science, Changchun Institute of Technology, Changchun, 130012, China

<sup>3</sup>State Key Laboratory of Luminescence and Applications, Changchun Institute of Optics, Fine Mechanics and Physics, Chinese Academy of Sciences, Changchun 130033, People's Republic of China

E-mail: [lw771119@hotmail.com](mailto:lw771119@hotmail.com), [lixuesong@ccut.edu.cn](mailto:lixuesong@ccut.edu.cn)

Fax: +86-0431-85716426; Tel: +86-0431-85716421

\* To whom all correspondence should be addressed.

## Experimental part

### 1.1. Photothermal performance test

The sunlight simulator is used to simulate the light source, the solar power meter is used to measure different light intensities, and the surface temperature of the coating is recorded by an infrared camera.

## 1.2 Passive anti-icing and active photothermal de-icing test

### 1.2.1 Icing delay test

The coated samples were placed on a cooling table at  $-15\text{ }^{\circ}\text{C}$  and the humidity of  $35\pm 5\%$ , and then  $15\text{ }\mu\text{l}$  of water was dropped onto the surface with a pipette gun. The freezing time began when the droplet temperature dropped to  $0\text{ }^{\circ}\text{C}$  and ended when the droplet was completely frozen.

### 1.2.2 Photothermal de-icing test

$30\text{ }\mu\text{l}$  and  $300\text{ }\mu\text{l}$  drops of water were placed at the coating surface. and frozen into ice on the cooling table at  $-15\text{ }^{\circ}\text{C}$ , and the de-icing process was recorded with an infrared camera; the coating was placed on the bottom of the petri dish, and the appropriate amount of water was added and placed in the refrigerator to form a  $2\text{ mm}$  ice layer, and the de-icing test was simulated with a light source.

## 1.3 Mechanical durability test

High and low temperature resistance: The coatings were first placed in a cryogenic bath at  $-70\text{ }^{\circ}\text{C}$  for  $6\text{ h}$ , next placed in a muffle furnace at  $200\text{ }^{\circ}\text{C}$  for  $48\text{ h}$ , and then tested for WCA and WSA at intervals.

Liquid Nitrogen Test: The coating was placed directly into liquid nitrogen for  $30\text{ min}$ , and the WCA and WSA were tested several times during this period.

Acid, alkali and salt solution immersion: The WCA and WSA of the coatings were determined after immersing the samples in  $\text{pH} = 1\text{ HCl}$  solution,  $\text{pH} = 14\text{ NaOH}$  solution and  $3.5\text{ wt}\%$   $\text{NaCl}$  solution.

Sand washing: The quartz sand washing test was performed according to ASTM D968-15.  $300\text{ mesh}$  sand was poured from the abrasion tester at a rate of  $50\text{ ml}$  per second.

Water flow washing: The water droplet impact test was conducted by simulating artificial rainfall, in which a continuous flow of water fell from a height of  $30\text{ cm}$  and impacted the surface of the sample inclined at  $45^{\circ}$ . The coating was then tested for WCA and WSA.

Sandpaper abrasion:  $360\text{ grit}$  sandpaper was arranged horizontally on the working table with the coated surface in contact with the sandpaper. A  $200\text{ g}$  weight was placed on the test specimen ( $4\text{ cm}^2$  area,  $5\text{ kPa}$  pressure) and pulled horizontally to move it at a speed of  $1\text{ cm/s}$ .

UV irradiation: Place the coating at a distance of  $50\text{ cm}$  below a  $40\text{ W}$  UV light. The wavelength spectrum of the UV light is  $185\text{-}500\text{ nm}$ . The coating was continuously irradiated for  $84\text{ h}$ .

Sonication: The coating was sonicated in an ultrasonic cleaner for  $5\text{ h}$  and the surface was observed whether the coating was peeling off or not, and WCA and WSA were measured at the same time.

Tape Peeling: 3M tapes were used to evaluate internal adhesion and adhesion to the substrate. Surface properties were evaluated by repeatedly applying and peeling the coated surface as well as measured the WCA and WSA of the coating after a fixed number of passes.

Impact resistance test: The superhydrophobic coating was sprayed on a polished aluminum plate, the aluminum substrate was fixed in a bracket hollowed out at the bottom, and the test was carried out using an impact resistance tester. Changes of the coating surface were recorded after repeated impacts of steel balls of the same mass (20 g) dropped from the same height (100 cm).

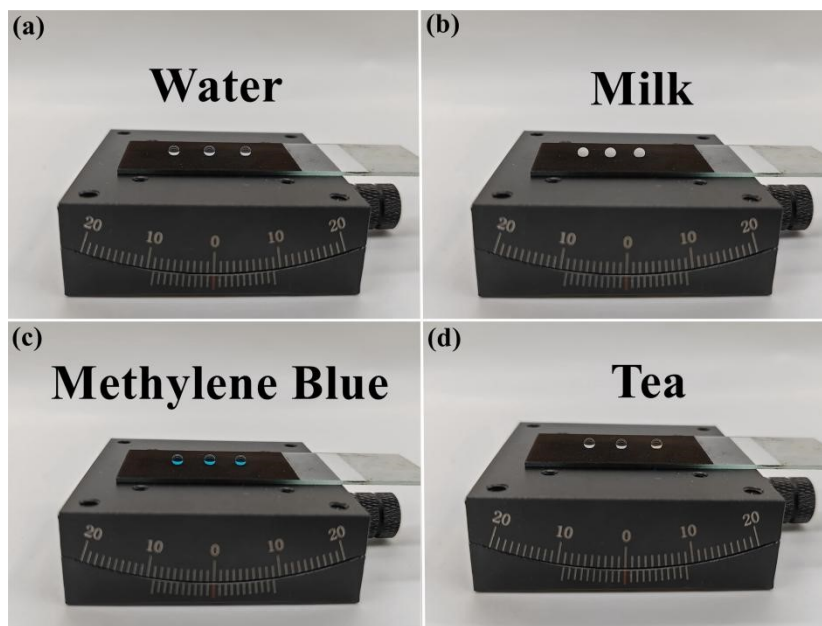


**Fig. S1.** Hydrophobic optical images of different liquids on the layers (a) water; (b) milk; (c) methylene blue; (d) tea.

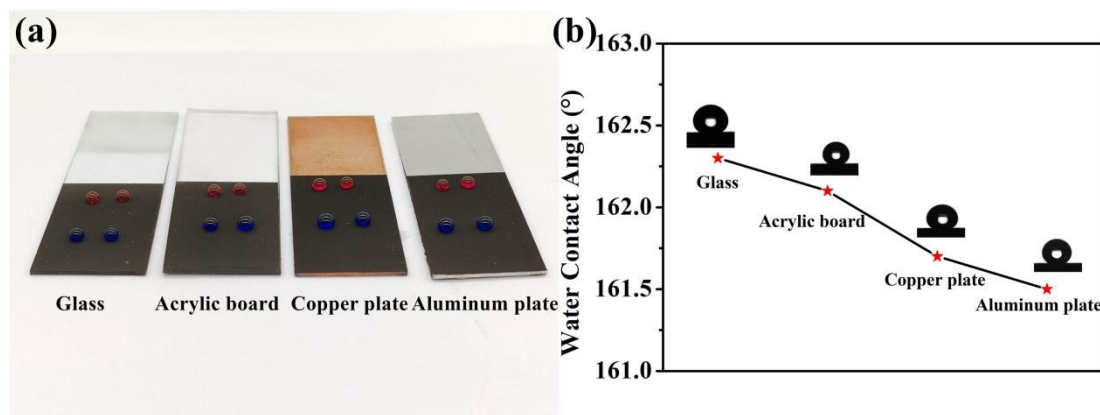


**Fig. S2.** (a) Hydrophobic optical images of different substrates (glass, acrylic board, copper plate, aluminum plate); (b) WCA of different substrates.

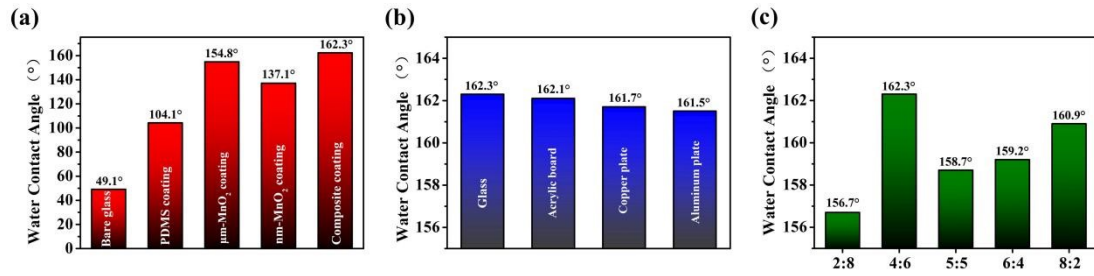


**Fig. S3.** Histograms of WCA (a) different coating materials on glass substrates; (b) substrates of different materials; (c) different mass ratios of  $\text{MnO}_2$ .

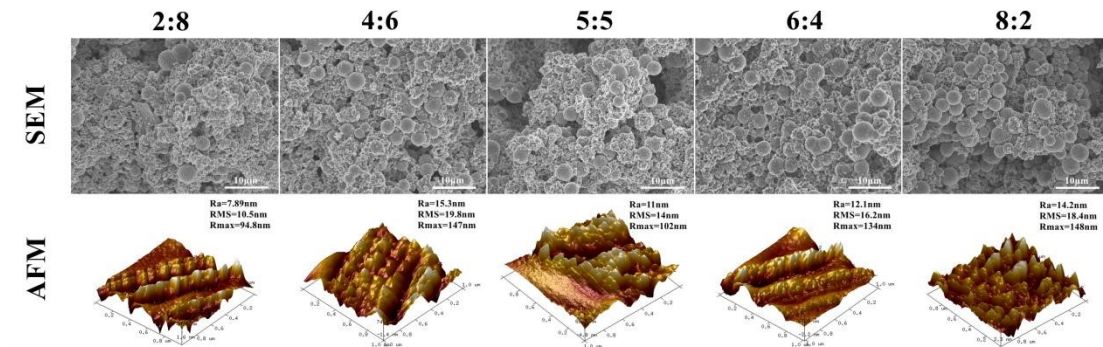


**Fig. S4.** SEM and AFM of  $\text{MnO}_2$  with different mass ratios ( $m_{\mu\text{m}}:m_{\text{nm}}$ ).

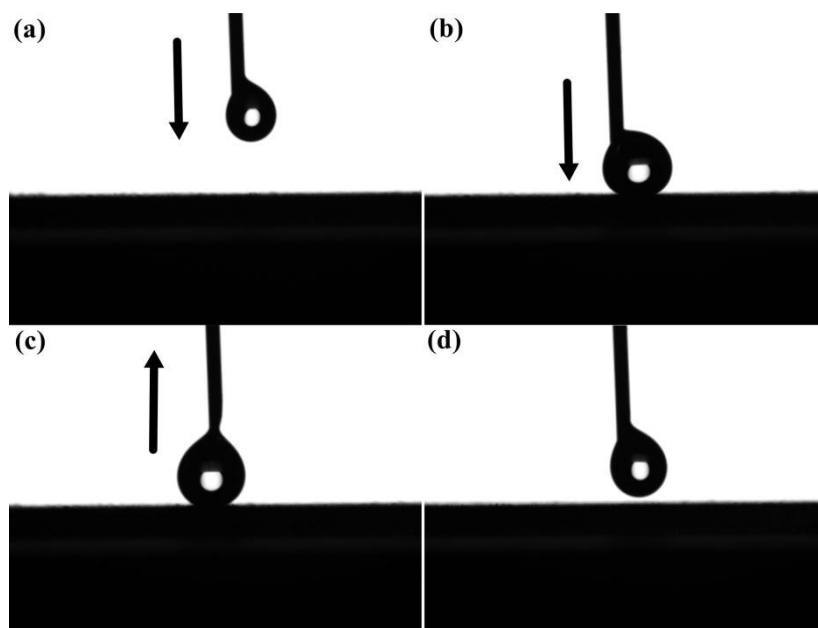


**Fig. S5.** Liquid droplets contact and detach from the coating surface during downward pressure and lifting.

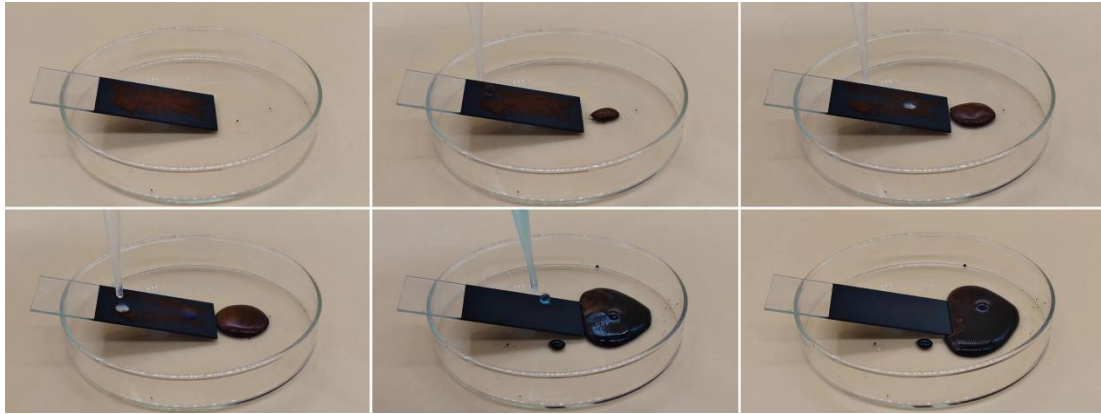


**Fig. S6.** Methylene blue dye simulates the self-cleaning process of dust.

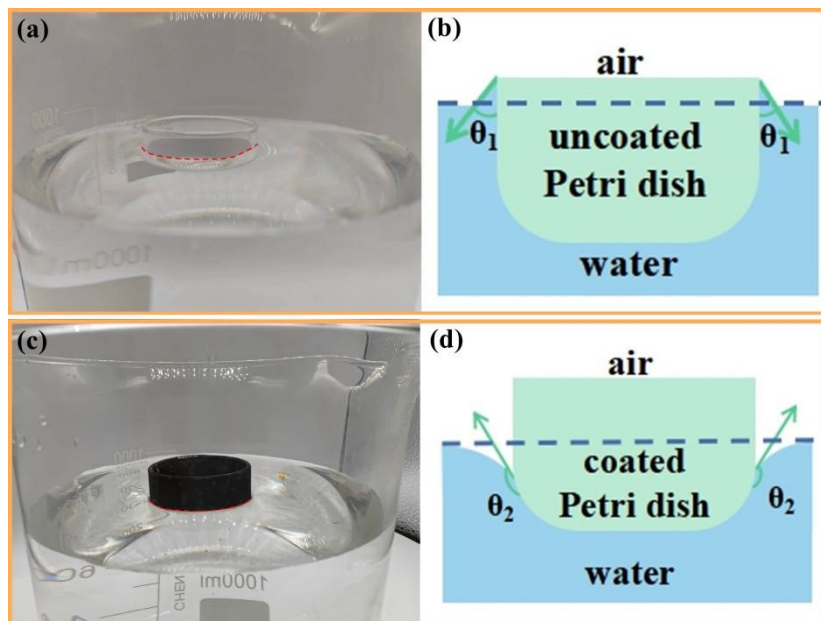


**Fig. S7.** Schematic of coated/uncoated petri dish in water and schematic of water surface tension.



**Fig. S8.** (a) Silver mirror phenomenon in water for coated petri dishes; (b) Carrying capacity test for uncoated petri dishes; (c) Carrying capacity test for coated petri dishes.

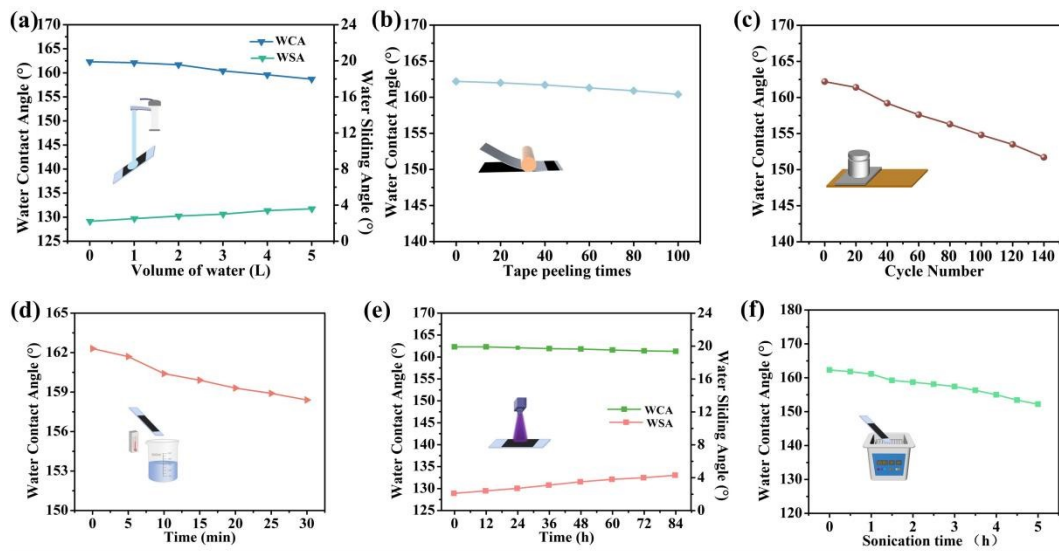


**Fig. S9.** (a) Water washing test; (b) Tape peeling test; (c) Sandpaper abrasion test; (d) Liquid nitrogen test; (e) Ultraviolet light irradiation test; (f) Sonication test.

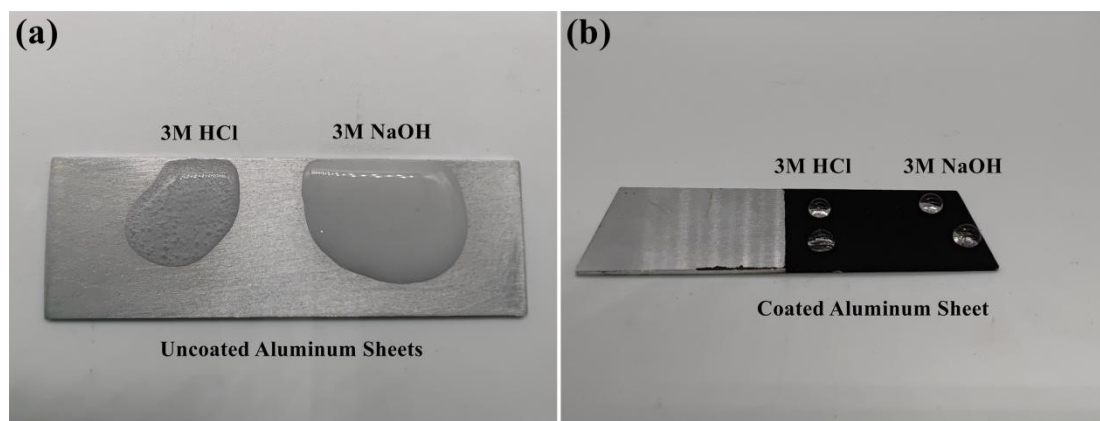


**Fig. S10.** Surface corrosion resistance test to acid and alkali solutions. (a) Uncoated aluminum plate; (b) Coated aluminum plate.

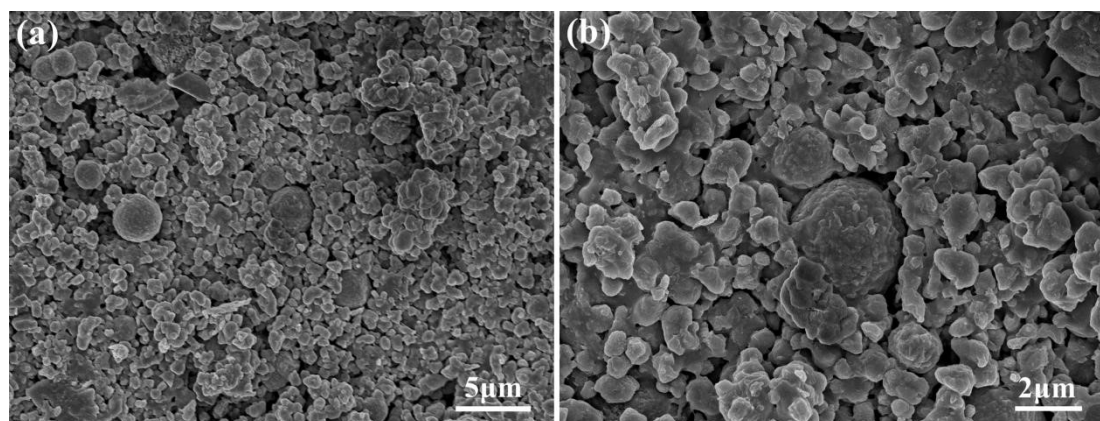


**Fig. S11.** SEM of coating changes after sandpaper abrasion.

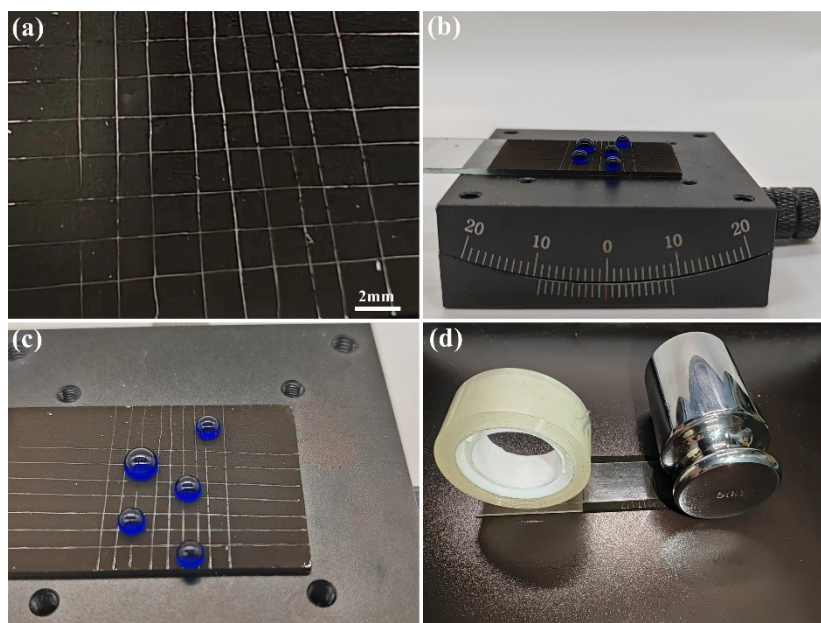


**Fig. S12.** (a) Grid lines on the coating surface after cutting; (b) Hydrophobicity of the coating after cutting; (c) Detailed image of the hydrophobicity; (d) Tape peel test after cutting.

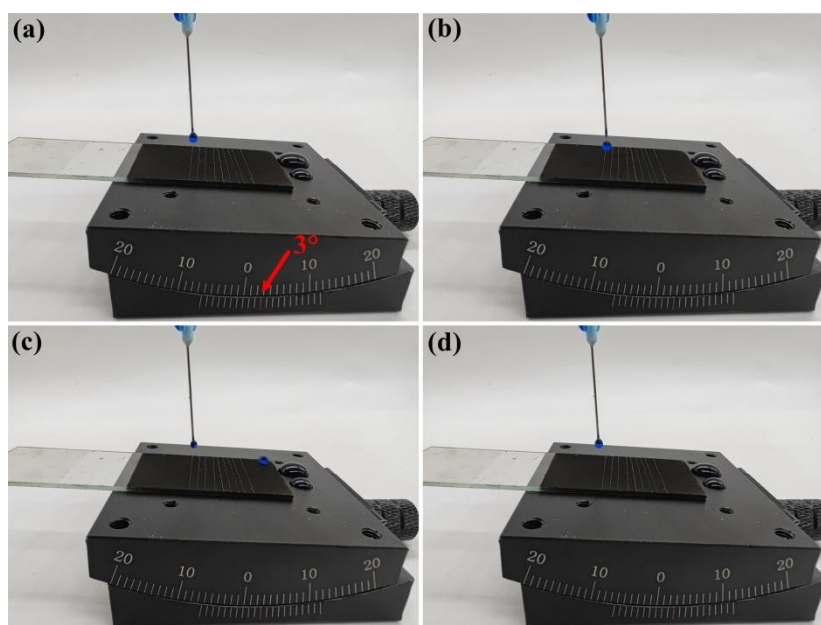


**Fig. S13.** Hydrophobicity test of the coating at small angle platform after cutting.

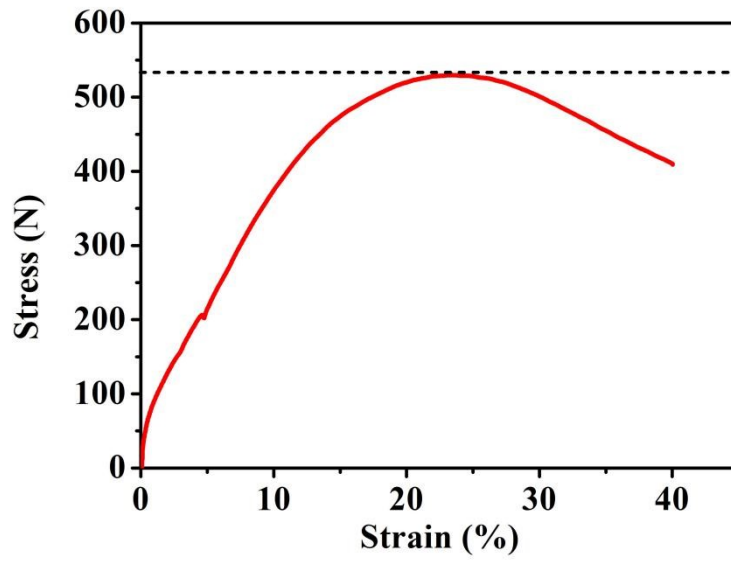


**Fig. S14.** Adhesion stretching curve between PDMS and glass.

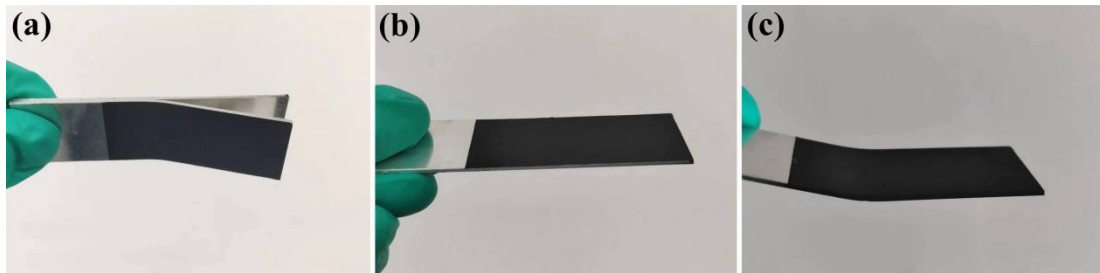


**Fig. S15.** Impact performance test (a) Comparison before and after steel ball impact; (b) Coating surface before steel ball impact; (c) Coating surface after steel ball impact.

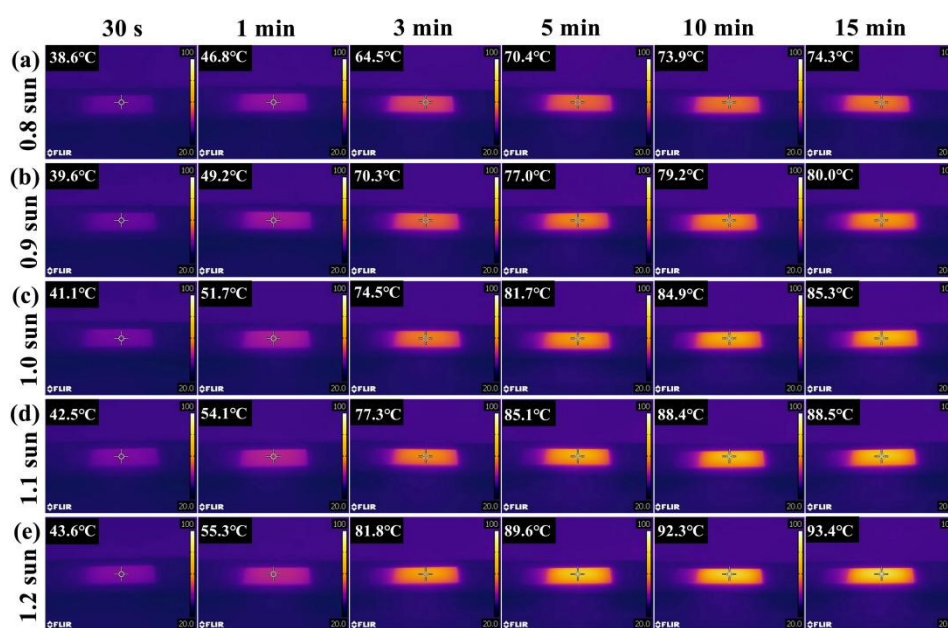


**Fig. S16.** Temperature variation of the coating surface under different light intensities (a) 0.8 sun; (b) 0.9 sun; (c) 1.0 sun; (d) 1.1 sun; (e) 1.2 sun.

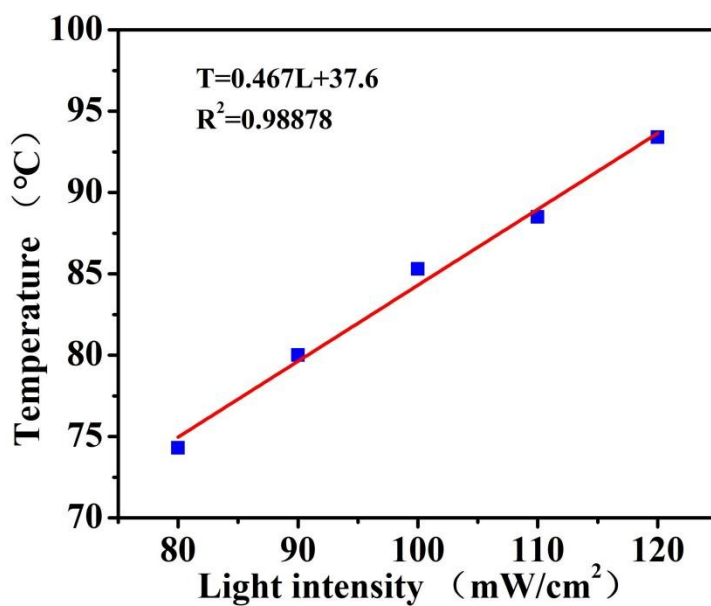


**Fig. S17.** Fitted curves and equations for the variation of coating surface temperature with light intensity.

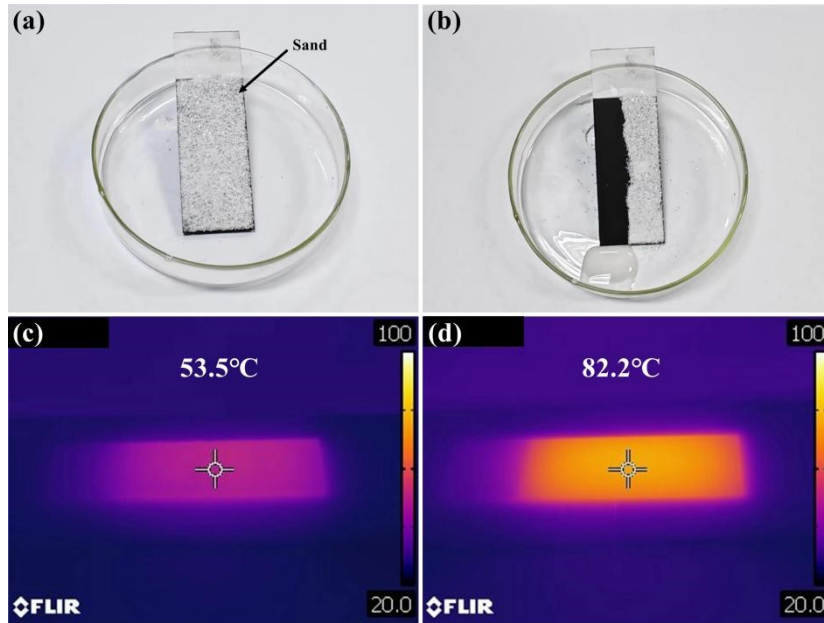


**Fig. S18.** Self-cleaning properties and IR temperature images of coatings at 1 sun intensity.

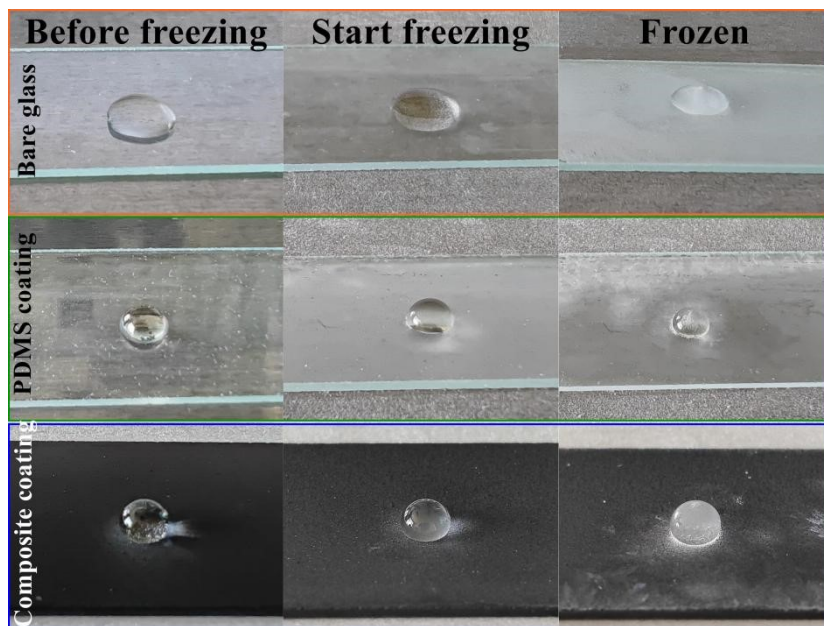


**Fig. S19.** The change process of water droplets during the whole freezing process.

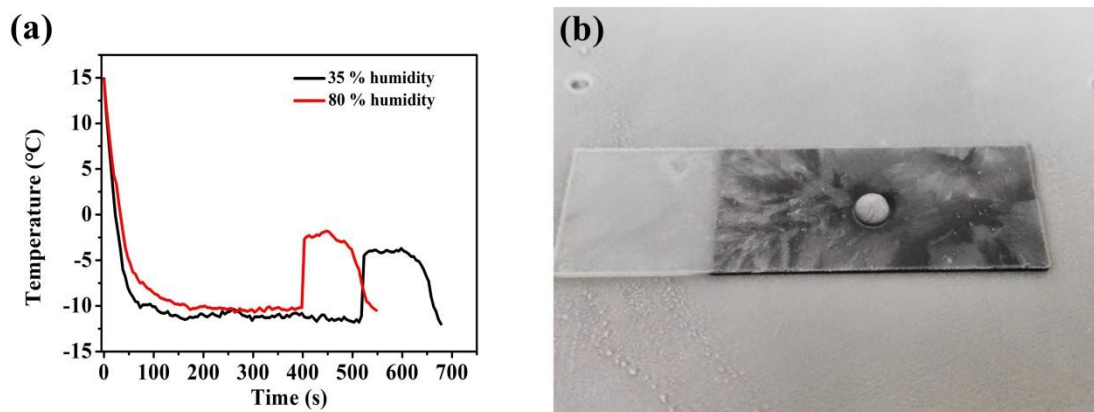


**Fig. S20.** (a) Freezing time in different humidity environments; (b) Coated surface after freezing in high humidity environments.

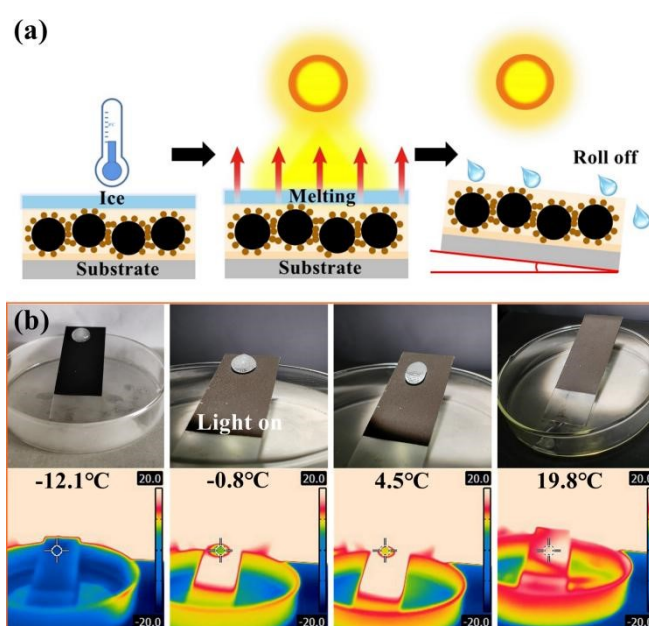


**Fig. S21.** (a) Schematic of a water droplet melting and rolling down on an inclined surface; (b) Melting process of a 300 µl water droplet at 1 sun intensity at an inclined angle.

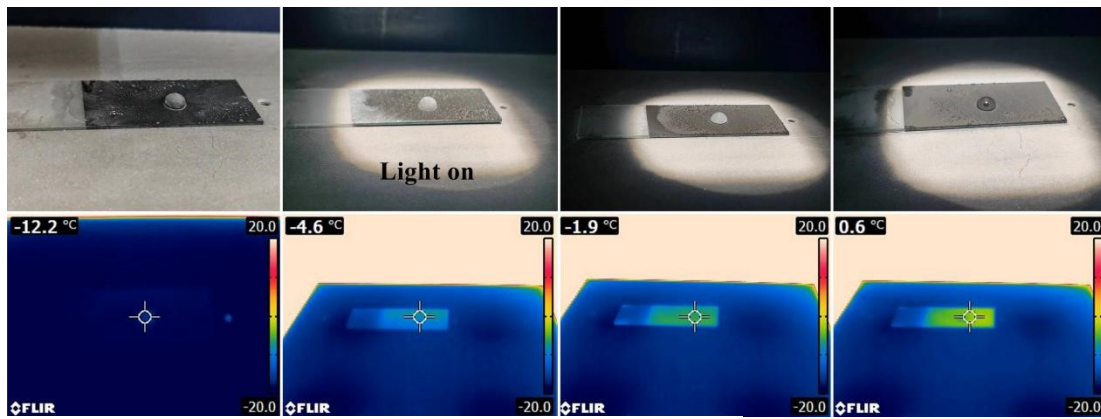


**Fig. S22.** The process of melt 30  $\mu\text{l}$  droplets at 0.8 solar intensity.



**Fig. S23.** Hydrophilicity of the original fabric and hydrophobicity of the coated fabric.



**Fig. S24.** Comparative images of commercial white fabrics, commercial black fabrics, and coated fabrics.

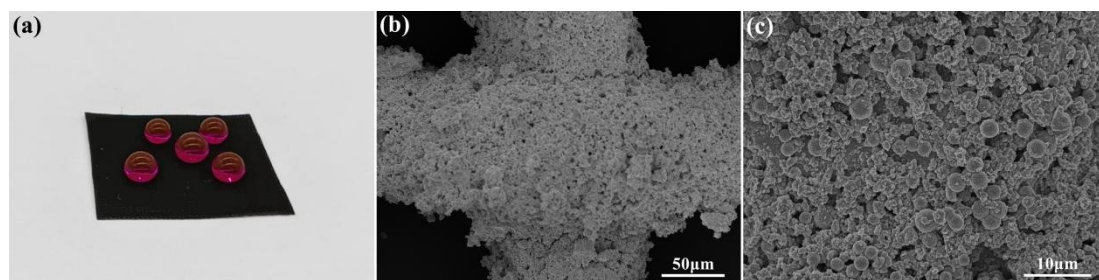


**Fig. S25.** (a) Hydrophobicity of water droplets on coated stainless steel mesh; (b) low magnification SEM of the coated stainless steel mesh surface; (c) high magnification SEM of the coated stainless steel mesh surface.

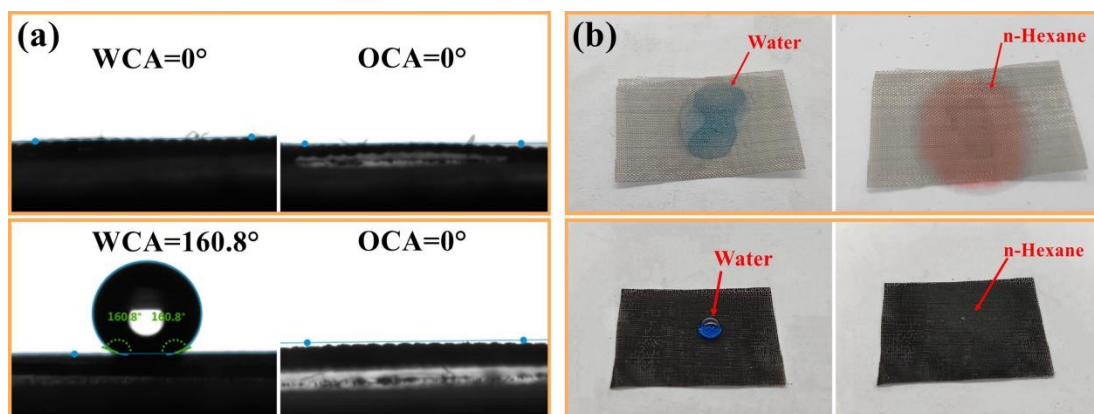


**Fig. S26.** (a) WCA and OCA of stainless steel mesh before and after coating; (b) Physical diagrams of lipophilicity and hydrophobicity of stainless steel mesh before and after coating.

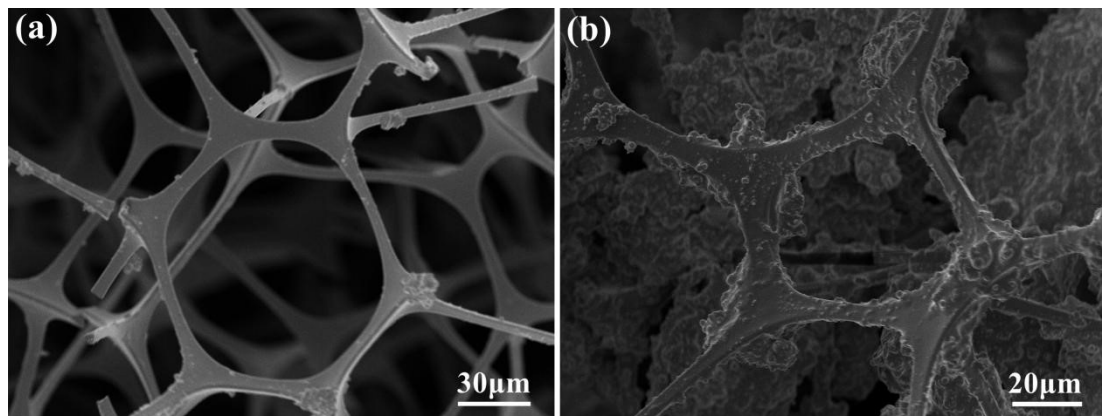


**Fig. S27.** SEM of the sponge before and after spraying.

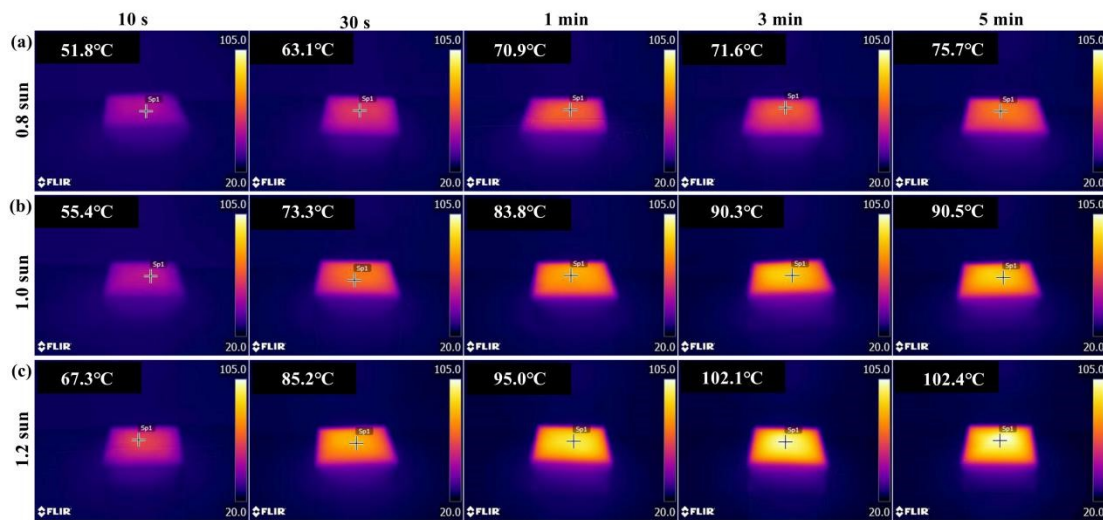


**Fig. S28.** Temperature variation of sponge surface in dry environment (air) under different light intensities.

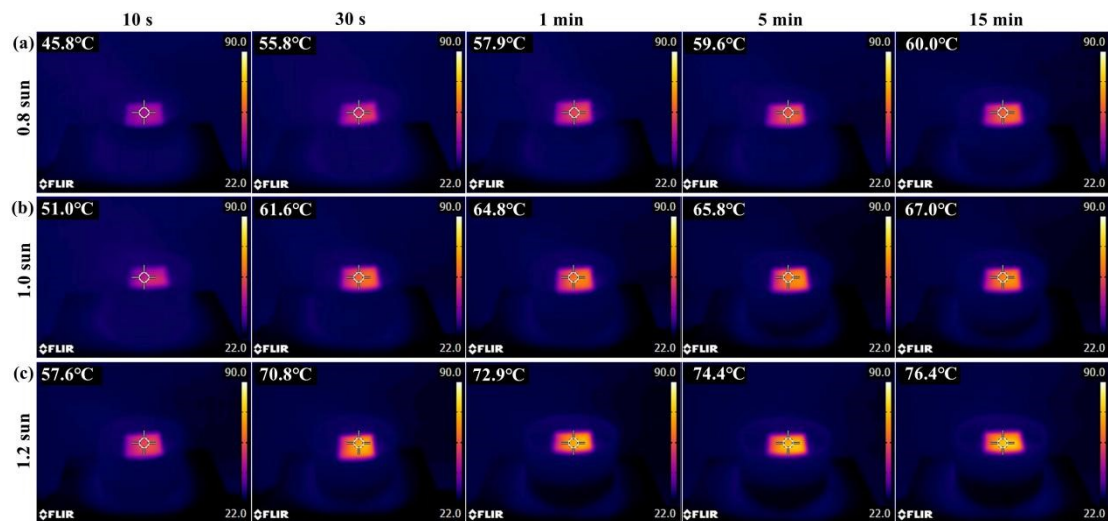


**Fig. S29.** Temperature variation of sponge surface in a wet environment (water) at different light intensities.

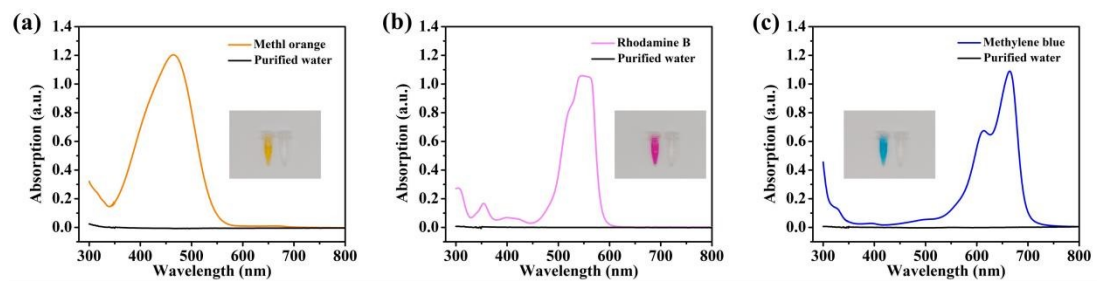


**Fig. S30.** UV characteristic absorption peaks and physical images of dyes before and after evaporation, (a) methyl orange; (b) rhodamine B; (c) methylene blue.